A STUDY ON TWO-SIDED LINEAR PREDICTION APPROACH FOR LAND MINE DETECTION

Thomas C. T. Chan[*], *H. C. So*[*] *and K. C. Ho*[†]

[*]Department of Electronic Engineering, City University of Hong Kong
Tat Chee Avenue, Kowloon, Hong Kong
[†]Department of Electrical and Computer Engineering, University of Missouri-Columbia
Columbia, MO 65211, USA

Index Terms – land mine detection, linear prediction, ground penetrating radar

ABSTRACT

Ground penetrating radar (GPR) is a widely used tool for land mine detection. However, land mine detection still remains a difficult task because of the changing conditions and the strong reflection of the ground. In this paper, a generalized two-sided linear prediction model is used to estimate the background. By effectively removing the background components from the GPR signal, the residual energy is found to be more reliable to generate the test statistic for detection. Results based on real GPR data show that the proposed method is able to not only remove the ground bounce and background signal but also suppress the response from some clutter objects.

1. INTRODUCTION

Since World War II, numerous conflicts in Europe, Africa, Central and South America, the Middle East and Asia resulted in the planting of millions of land mines. It is important to locate these mines that can potentially cause massive number of deaths and casualties.

Owing to the capabilities of good penetration and depth resolution as well as detecting both metallic and nonmetallic objects, ground penetrating radar (GPR) [1]-[3] has been considered as a viable technology for land mine detection. A GPR system consists of a transmitter for emitting electromagnetic wave to the inspection surface and a receiver for collecting the returned signal from which the decision of whether there is a mine is made. However, detecting land mines with GPR is still a difficult task because on one hand environmental conditions such as soil type and moisture content and strong reflections from the ground surface, namely, ground bounce, can make the returned signals from the background interference and mine very similar. On the other hand, the land mine signatures are inconsistent and they vary according to their depths, types, etc. As a result, signal processing is a crucial step for rendering the GPR sensor outputs to increase probability of detection and/or reduce false alarm rate. In [4], it is suggested to remove the ground bounce by modelling it as a shifted and scaled version of an adaptively estimated reference ground bounce, while [5] proposes to use to a constant false alarm rate detector via modelling the background component by a time-varying linear prediction (LP) function. A Kalman filter based approach for mine detection has been proposed by Zoubir *et al* [6]. Recently, Ho *et al* [7] have proposed to use the frequency domain features from the GPR signals to improve detection of weak mines and to reduce false alarms due to clutter objects. In this paper, we extend the LP idea of [5] to enhance detection performance. Unlike [5] which processes GPR signal in frequency domain with one-sided LP modelling, we propose the use of a two-sided LP model [8] and perform processing in spatial domain.

The rest of the paper is organized as follows. Our proposed method will be presented in Section 2. Experimental results are shown in Section 3, and concluding remarks are drawn in Section 4.

2. PROPOSED METHOD

In our study, we have investigated the GPR data sets from [9]. The GPR data are obtained by measuring the response from an impulse GPR with a center frequency of around 1GHz in the time domain. Each setup contains land mines and other objects including large stone, empty cartridge, and/or copper wire strip. A typical setup is shown in Figure 1. For each y, denoted as channel, the operator sweeps the GPR device along the x direction, recording a response in every 1 cm apart. A total of 51 channels, separated by 1 cm in space, along with 196 measurements per channel, denoted as scans, complete a GPR data set for a setup. Each GPR response, $\mathbf{d}(x,y)$, has a total of 512 samples with a sampling interval of 25 ps. The B-scan of the 25th channel for the setup in Figure 1 is shown in Figure 2 where the horizontal axis and vertical axis correspond to the scan number and depth, respectively. Hot colours represents positive magnitudes while Cool colours represent negative magnitudes. The blue line seen in Figure 2 represents the initial ground surface's response.

Given a GPR A-scan response vector $\mathbf{d}(x,y)$ where x and y represent the dimensions of scan and channel, respectively, the task of land mine detection can be casted as the following binary hypothesis test:

$$\begin{aligned} H_0 &: \mathbf{d}(x,y) = \mathbf{g}(x,y) + \mathbf{q}(x,y) \\ H_1 &: \mathbf{d}(x,y) = \mathbf{s}(x,y) + \mathbf{g}(x,y) + \mathbf{q}(x,y) \end{aligned} \tag{1}$$

where $\mathbf{g}(x,y)$ represents the background response, which is the composite of the surface and/or clutter response, $\mathbf{q}(x,y)$ denotes measurement noise at the GPR antenna, and $\mathbf{s}(x,y)$ is the response from a land mine. That is, we assume that $\mathbf{d}(x,y)$ is a linear combination of $\mathbf{g}(x,y)$ and $\mathbf{q}(x,y)$, and also $\mathbf{s}(x,y)$ if a mine is present. In practical situation, the GPR data are collected at very high signal-to-noise ratio and thus the effect of $\mathbf{q}(x,y)$ is negligible, while the background is the dominant response in both hypotheses.

The basic assumption of our proposed methodology is that $\mathbf{g}(x,y)$ can be modelled using LP while $\mathbf{s}(x,y)$ cannot. This idea is in fact adapted from [5] and experimental results in Section III demonstrate the improvement of our proposal. We will first subtract an estimate of $\mathbf{g}(x,y)$ formed by using LP model from the GPR signal. Then the power of the residual signal will be utilized to decide if each location, (x,y), falls under H_0 or H_1.

2.1 Background Modelling

Since the background is highly correlated in space, a simple LP model adapted from [5] can be used for $\mathbf{g}(x,y)$:

$$\mathbf{g}(x,y) = a_p(x)\ \mathbf{g}(x-p,y) + \mathbf{e}(x,y) \tag{2}$$

where $a_p(x)$ is the LP coefficient and $\mathbf{e}(x,y)$ denotes the unknown modelling error. The problem is that $\mathbf{g}(x-p,y)$ must be known for our estimation. An assumption can be made that the past location always falls under H_0, that is $\mathbf{d}(x-p,y) = \mathbf{g}(x-p,y) + \mathbf{q}(x-p,y)$, then it is reasonable to replace $\mathbf{g}(x-p,y)$ with $\mathbf{d}(x-p,y)$:

$$\mathbf{g}(x,y) \approx a_p(x)\ \mathbf{d}(x-p,y) \tag{3}$$

However, $x-p$ could fall under H_1, and thus the estimation of $\mathbf{g}(x,y)$ using (4) will become meaningless. An alternative is to estimate $\mathbf{g}(x,y)$ with

$$\mathbf{g}(x,y) \approx a_p(x)\ \hat{\mathbf{g}}(x-p,y) \tag{4}$$

by initially setting

$$\hat{\mathbf{g}}(x_0,y) = \mathbf{d}(x_0,y) \tag{5}$$

with the knowledge that location x_0 is under H_0. This, however, will cause a propagation in error with $\mathbf{e}(1,y), \mathbf{e}(2,y), ..., \mathbf{e}(x,y)$, and ignore the variation in the background.

Another concern rises when (2) does not provide an accurate estimate of $\mathbf{g}(x,y)$ due to step changes in the background, for example, the interference of a large clutter object. A more accurate way to estimate $\mathbf{g}(x,y)$ is to use a conventional two-sided LP model [8]:

$$\begin{aligned} &\mathbf{g}(x,y) = \\ &a_p(x)\ (\mathbf{g}(x-p,y) + \mathbf{g}(x+p,y)) + \mathbf{e}(x,y) \end{aligned} \tag{6}$$

and approximating $\mathbf{g}(x,y)$ with

$$\mathbf{g}(x,y) \approx a_p(x)\,(\mathbf{d}(x-p,y) + \mathbf{d}(x+p,y))\,. \tag{7}$$

With the two-sided LP model in (7), a more accurate estimation of $\mathbf{g}(x,y)$ is expected because samples from both the past, $\mathbf{d}(x-p,y)$, and the future, $\mathbf{d}(x+p,y)$, are used. However, (7) will not be a good approximation of (6) when either location, $x-p$ or $x+p$, falls under H_0.

To solve the problem present in both (2) and (6), we propose to estimate the background $\mathbf{g}(x,y)$ using a generalized two-sided LP model:

$$\begin{aligned} &\mathbf{g}(x,y) = \\ &a_{p_-}(x)\ \mathbf{g}(x-p,y) + a_{p_+}(x)\ \mathbf{g}(x+p,y) + \mathbf{e}(x,y) \end{aligned} \tag{8}$$

where $a_{p_-}(x)$ is not necessarily equal to $a_{p_+}(x)$ as in the conventional case. The background $\mathbf{g}(x,y)$ is then approximated as

$$\mathbf{g}(x,y) \approx a_{p_-}(x)\ \mathbf{d}(x-p,y) + a_{p_+}(x)\ \mathbf{d}(x+p,y) \tag{9}$$

With our proposed model, by allowing $a_{p_-}(x)$ to differ from $a_{p_+}(x)$, the estimation will be very accurate as long as one of the two locations, $x-p$ or $x+p$, falls under H_0. Clutter objects that are larger in size than typical land mines will also not result in a wrong estimate of the background by setting p approximating the size of typical land mines. The two-sided LP model requires a lookahead of p scans. The lookahead is often tolerable in vehicle-mounted GPR platform because the GPR sensor is in the front of the vehicle and a decision does not need to be made until the tail of the vehicle passes through the inspected location.

2.2 Background Estimation and Elimination

Denoting

$$\mathbf{D}_p(x,y) = [\mathbf{d}(x-p,y)\ \mathbf{d}(x+p,y)]^T \tag{10}$$

and

$$\mathbf{a}_p(x) = [a_{p_-}(x)\ a_{p_+}(x)]^T, \tag{11}$$

(9) can be rewritten as

$$\mathbf{g}(x,y) \approx \mathbf{D}_p^T(x,y,z)\ \mathbf{a}_p(x) \tag{12}$$

The estimate of $\mathbf{a}_p(x)$, denoted by $\hat{\mathbf{a}}_p(x)$, is computed using standard least squares as

$$\hat{\mathbf{a}}_p(x) = \left(\mathbf{D}_p(x,y)\mathbf{D}_p^T(x,y)\right)^{-1}\mathbf{D}_p(x,y)\mathbf{d}(x,y) \quad (13)$$

The estimated background then becomes

$$\hat{\mathbf{g}}(x,y) = \mathbf{D}_p(x,y)\hat{\mathbf{a}}_p \quad (14)$$

Figure 3 shows the estimation of the background of the three models, one-sided LP of (3), conventional two-sided LP of (7), and the generalized two-sided LP of (9) in the scenario where the location x is under H_0, $x-p$ contains a mine and $x+p$ does not ($x=40$, $y=25$, $p=10$ for the setup shown in Figure 1). It can be seen clearly that the estimated background using (9) is much more accurate. Although the computation complexity increases, it ensures that the the estimation of the background follows the LP model in (8) correctly.

The background of the signal can then be eliminated by subtracting the estimated background $\hat{\mathbf{g}}(x,y)$from $\mathbf{d}(x,y)$ leaving the residual signal denoted by $\mathbf{h}(x,y)$:

$$\mathbf{h}(x,y) = \mathbf{d}(x,y) - \hat{\mathbf{g}}(x,y) \quad (15)$$

2.3 Generating Test statistic

With the assumption that the background is correctly estimated, our detection task reduces to the following hypothesis:

$$\begin{aligned} H_0 &: \mathbf{h}(x,y) = \mathbf{q}(x,y) \\ H_1 &: \mathbf{h}(x,y) = \mathbf{s}(x,y) + \mathbf{q}(x,y) \end{aligned} \quad (16)$$

It is expected that the energy of $\mathbf{h}(x,y)$ will be much larger under H_1 than in the case of H_0. As a result, the residual energy is utilized in producing the test statistic, which is given by the average of the residual energy in the vicinity of a suspected scan location, x:

$$\varepsilon(x,y) = \frac{1}{N}\sum_{n=y-\frac{N-1}{2}}^{y+\frac{N-1}{2}} \mathbf{h}(x,n)^T\mathbf{h}(x,n) \quad (17)$$

where N is the span of channels to be averaged and its choice depends on the size of the suspected mines, and x and y is the inspected scan location and channel, respectively. By setting the target area comparable to size of land mines, we can eliminate the false detection from clutter objects that are smaller in size and lie on the inspected channel.

3. EXPERIMENTAL RESULTS

The proposed method was tested on the setup in Figure 1. The objects, namely, the PMA-3 mine, large stone, PMA-1 mine, and copper strip were centered on the 25th, 75th, 125th, and 175th scan, respectively, and were buried 5 cm deep in clay mixed with small rocks. Furthermore, all of the objects were centered on the 25th channel. The GPR data were collected after 23 days with the clay still moist. In our study, $p=10$ and N was set to 9. After processing with our proposed method, $\varepsilon(x,y)$ was computed and projected onto a 2-D image and is shown in Figure 4. The bright spots represents the regions where the mines are located. We can clearly see the two mines in the figure although the PMA-3 mine is more obvious. For comparison, $\varepsilon(x,25)$ was also plotted against x in Figure 5. Other background removal algorithms, namely, the one-sided LP model, the conventional two-sided LP model, and the adaptive ground bounce removal (AGBR) algorithm in [4] are also shown for comparison. y was set to 25 because the suspected mines were centered on the 25th channel. It is seen that the generalized and conventional two-sided LP schemes were able to remove the effect of the background and all clutter objects while the other two methods would detect a false alarm with the copper strip (at $x=170$ to 190). The proposed method is also more preferable than the conventional two-sided LP because undesirable multiple peaks are not present around the mines.

Another setup from [9], shown in Figure 6, was also tested. Basically, this setup is similar to Figure 1 except that an empty cartridge case replaced the large stone on the 75th scan. The GPR data were acquired when the clay was hard and dry. The value of $\varepsilon(x,25)$ was again plotted against x, and compared with other methods and the results are shown in Figure 7. Our proposed method once again proved superior in suppressing the response of the copper strip from the GPR data.

4. CONCLUSION

A generalized two-sided linear prediction (LP) method has been proposed to eliminate the background from a GPR response. In effectively removing of the response of the ground surface and other clutter objects, the response from mines can be extracted. Our proposed method is superior in performance to the adaptive ground bounce removal and conventional LP modelling algorithms. Future research will be focused on modelling the mine response so that we can differentiate better the response between mines and clutter objects. The geometry and depth of the mine response will also be explored for enhancing detection performance.

Acknowledgement

The work described in this paper was fully supported by a grant from the Research Grants Council of the Hong Kong Special Administrative Region, China [Project No. CityU 119605].

REFERENCES

[1] L. Peter, Jr., J.J. Daniel and J.D. Young, "Ground penetrating radar as a subsurface environmental sensing tool," *Proc. IEEE*, vol.82, pp.1802-1822, Dec. 1994

[2] D.J. Daniels, *Surface-Penetrating Radar*, London: Institution of Electrical Engineers, 1996

[3] T.R. Witten, "Present state of the art in ground-penetrating radars for mine detection," *Proc. SPIE Conf.*, vol.3392, pp.576-586, Orlando, FL, 1998

[4] R. Wu, A. Clement, J. Li, E.G. Larsson, M. Bradley, J. Habersat and G. Maksymonko, "Adaptive ground bounce removal," *Electronics Letters*, vol.37, no.20, pp.1250-1252, Sept. 2001

[5] K.C. Ho and P.D. Gader, "A linear prediction land mine detection algorithm for hand held ground penetrating radar," *IEEE Trans. Geosci. Remote Sensing*, vol. 40, no.6, pp.1374-1384, June 2002

[6] A.M. Zoubir, I.J. Chant, C.L. Brown, B. Barkat and C. Abeynayake, "Signal processing techniques for landmine detection using impulse ground penetrating radar," *IEEE Sensors Journal*, vol.2, no.1, pp.41-51, Feb. 2002

[7] K.C. Ho, P.D. Gader and J.N. Wilson, "Improving landmine detection using frequency domain features from ground penetrating radar," *Proc. IEEE International Conference on Geoscience and Remote Sensing Symposium*, vol.3, pp.1617-1620, 2004

[8] J.-J Hsue and A.E. Yagle, "Similarities and differences between one-sided and two-sided linear prediction," *IEEE Trans. Signal Processing*, vol.43, no.1, pp.345-349, Jan. 1995

[9] http://www.minedet.etro.vub.ac.be/groundbase/datafiles/html/datafiles.html

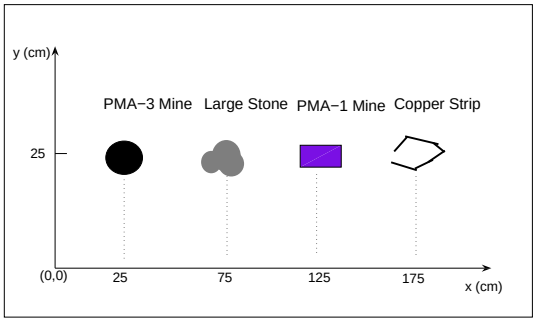

Figure 1: Setup 1 from [9]

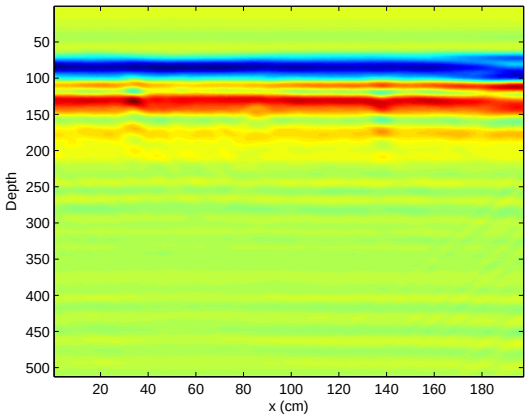

Figure 2: B-scan of GPR data

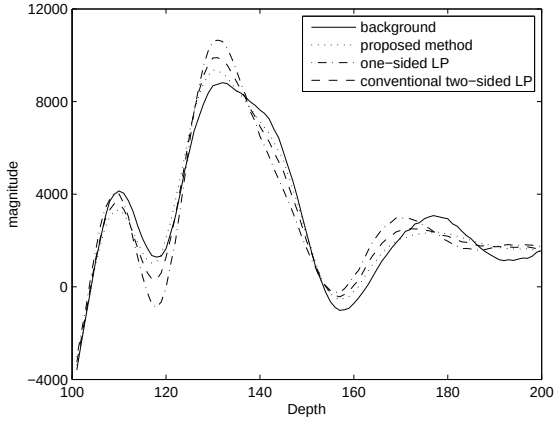

Figure 3: Estimated Background

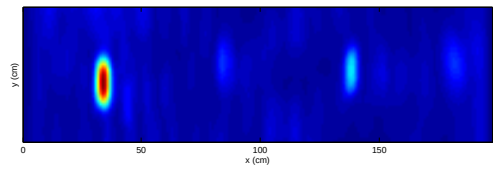

Figure 4: Residue energy projected onto a 2-D image

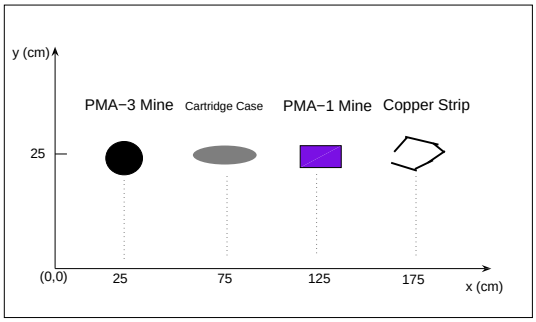

Figure 6: Setup 2 from [9]

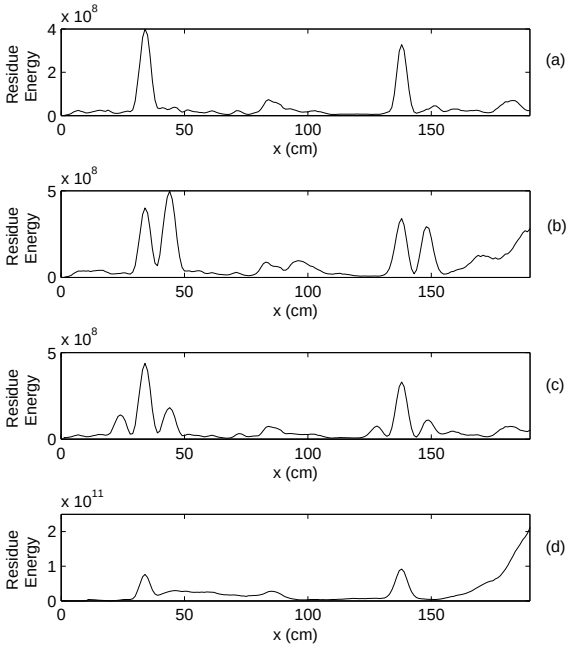

Figure 5: Residual energy versus scan location for Setup 1: (a) proposed method, (b) one-sided LP, (c) constrained two-sided LP, (d) AGBR

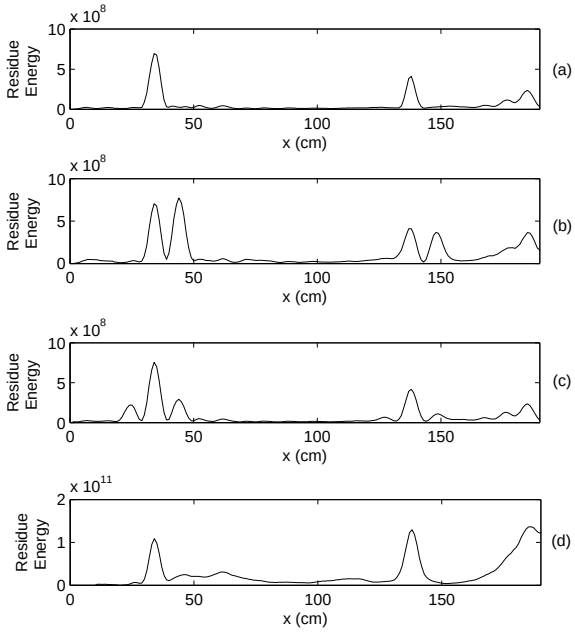

Figure 7: Residual energy versus scan location for Setup 2: (a) proposed method, (b) one-sided LP, (c) constrained two-sided LP, (d) AGBR